Metabolic Brain Disease (2019) 34:1385–1399
https://doi.org/10.1007/s11011-019-00444-x

ORIGINAL ARTICLE

Type 2 diabetes induced oxidative brain injury involves altered cerebellar neuronal integrity and elemental distribution, and exacerbated Nrf2 expression: therapeutic potential of raffia palm (*Raphia hookeri*) wine

Ochuko L. Erukainure[1,2] · Omamuyovwi M. Ijomone[3,4] · Olakunle Sanni[1] · Michael Aschner[3] · Md. Shahidul Islam[1]

Received: 25 November 2018 / Accepted: 28 May 2019 / Published online: 14 June 2019

Abstract

Neurodegenerative diseases, such as Alzheimer's disease have been recognized as one of the microvascular complications of type 2 diabetes (T2D). In this study, the effect of T2D on neuronal integrity and elemental distribution in the cerebellar cortex, as well as the therapeutic effect of Raffia Palm *(Raphia hookeri)* wine (RPW) were investigated in male albino rats. T2D was induced in 4 groups of rats using fructose and streptozotocin. One group served as negative control which was administered water, the second and third group were administered 150 and 300 mg/kg bodyweight of RPW, while the fourth was administered metformin (200 mg/kg bodyweight). Two other groups of normal rats were administered distilled water (control) and of RPW (300 mg/kg bodyweight). The rats were sacrificed after 5 weeks of treatment, and brains were collected. The cerebellum was removed, and several parts analyzed by immunochemistry, histology and scanning electron microscopy (SEM). Remaining brain tissues were used to analyze for the oxidative stress biomarkers and acetylcholinesterase activity. These analyses revealed oxidative damage with concomitantly increased acetylcholinesterase activity and upregulation of Nrf2 expression in the diabetic brain cerebellar cortexes. Histological and microscopic analysis also revealed altered distribution of neurons and axonal nodes with concomitant elevated levels of several heavy metals. Treatment with RPW significantly elevated glutathione (GSH) level, superoxide dismutase (SOD) and catalase activities, as well as depleted acetylcholinesterase and malondialdehyde (MDA) level and concomitantly inhibited Nrf2 expression. It also improved neuronal integrity and reduced the levels of heavy metals in brain. Taken together, the results of this study suggest that the RPW may afford a novel neuroprotective potential against diabetic neurodegeneration.

Keywords Raffia palm wine · Type 2 diabetes · EDX (Energy dispersive X-ray) · Neurodegeneration · Nrf2 expression

Introduction

Being a major global epidemic, diabetes mellitus (DM) is a metabolic disease characterized by increased blood glucose level due to the incapability of pancreatic β-cells to synthesize insulin as seen in type 1 diabetes (T1D) and/or insufficient utilization of synthesized insulin as seen in type 2 diabetes (T2D) (Unnikrishnan et al. 2017; van Crevel et al. 2017). T2D is the predominant of all DM types and it is characterized by insulin resistance and partial pancreatic β-cell dysfunction, leading to chronic hyperglycemia. Chronic hyperglycemia, in turn, leads to excess production of free radicals, which can initiate oxidative stress when they surpass the tissue's endogenous antioxidant capacity (Erukainure et al. 2017; Maritim et al. 2003). Hyperglycemia-induced oxidative stress has been associated with the pathogenesis and progression of micro- and macro- vascular complications in T2D.

Neurodegeneration has been recognized as one of the microvascular complications in T2D (Vagelatos and Eslick 2013; Whitlow et al. 2015; Wrighten et al. 2009), with oxidative stress

✉ Md. Shahidul Islam
islamd@ukzn.ac.za

[1] Department of Biochemistry, School of Life Sciences, University of KwaZulu-Natal, (Westville Campus), Durban 4000, South Africa

[2] Nutrition and Toxicology Division, Federal Institute of Industrial Research, Lagos, Nigeria

[3] Department of Molecular Pharmacology, Albert Einstein College of Medicine, New York, NY, USA

[4] Department of Human Anatomy, Federal University of Technology, Akure, Nigeria

playing a key role in mediating tis effect (Kim et al. 2015; Uttara et al. 2009). The brain utilizes glucose as its predominant source of energy, when glucose transporters transport it across the blood-brain barrier (BBB) (McEwen and Reagan 2004; Reagan et al. 2008; Wrighten et al. 2009). However, this homeostasis is disrupted in T2D due to impaired signaling and the down regulation of glucose transporters (GLUTs) (Gejl et al. 2017; Hwang et al. 2017; Pardridge et al. 1990; Wrighten et al. 2009), leading to neuronal loss, structural alterations, and metal accumulation (Folarin et al. 2017; Kim et al. 2015; Wrighten et al. 2009).

The role of nuclear factor erythroid 2–related factor 2 (Nrf2) has been correlated with redox homeostasis as it mediates the activation and recruitment of endogenous antioxidants in response to oxidative stress (Dieter 2014; Ma 2013). Its beneficial role has been reported in cerebellar function and neurodegenerative diseases such as Alzheimer and Parkinson (Ma 2013; Sandberg et al. 2014), cardiovascular diseases (Barančík et al. 2016), and hepatoxicity (Ma 2013). Its role in the activation of oxidative stress has been reported (Wrighten et al. 2009; Zucker et al. 2014). The activation of Nrf2 on the onset of T2D with concomitant generation of ROS, leading to downstream of antioxidants has also been reported (He et al. 2012; Miao et al. 2012).

Raffia palm (*Raphia hookeri*) wine (RPW) refers to the natural beverage obtained from the trunks of *Raphia hookeri* (raffia palm tree) (Eze and Ogan 1988b; Nwaiwu et al. 2016). Its consumption cuts across West Africa and Asia where it is utilized for spiritual, socio-economical and medicinal purposes. In traditional medicine, it is usually employed as a macerating medium for medicinal plants, but can be utilized singly. Its medicinal uses include treatment of measles, breast milk replenishment, and aphrodisiac (Gruca et al. 2014; Kosseva et al. 2016; Okwu and Nnamdi 2008; Rätsch 2005). Erukainure et al. (2019a, 2019b) reported the ability of RPW to reduce blood glucose level, oxidative stress and ameliorate testicular damage in diabetic rats. Its macro and micro – nutritional constituents, which consists of ascorbic acid, B vitamins, calcium, potassium, sodium, nitrogen and phosphorus have been reported (Bassir 1962; Cunningham and Wehmeyer 1988; Eze and Ogan 1988; Obahiagbon and Osagie 2007; Tuley 1965). Its phytochemical constituents have been reported to include hydroxycaffeic acid, luteic acid, caffeic acid, 7,4′-dihydroxyflavone, protocatechuic acid 4-glucoside, gallic acid 3-glucoside, flavogallol, gallocatechin gallate, 7,4′-dimethoxyflavone (Erukainure et al. 2018b). It has also been reported to be rich in the sugars: glucose, raffinose, sucrose, xylose, and lactose (Ezeagu et al. 2003; Obahiagbon and Osagie 2007). These sugars are not only responsible for its sweetness, but act as fermentation substrates for the high *Saccharomyces cerevisiae* content of RPW.

This study aims to investigate the effect of RPW on the redox status, ATPase and acetylcholinesterase activities in whole brain, as well as the morphology, neuronal distribution, elemental distribution, and Nrf2 expression in the cerebellar cortex of T2D rats. Brain glucose uptake has been reported to alter in T2D due to the down regulation of GLUTs (Gejl et al. 2017; Hwang et al. 2017; Pardridge et al. 1990), thus the ability of RPW to stimulate glucose uptake in brain tissues was also investigated ex vivo.

Materials and methods

Raffia palm wine

Raffia palm wine was obtained fresh from local palm tappers in Benin city, Nigeria. They were concentrated in a water bath at 50 °C and stored at 4 °C.

Experimental animals

Thirty eight male albino rats of Sprague-Dawley (SD) strain, weighing about 180–200 g were collected from the Biomedical Research Unit (BRU), University of KwaZulu-Natal, Durban, South Africa. The animals were maintained under optimum temperature and humidity with natural photo period of 12-h light-dark cycle, while acclimatizing on pelletized rat chows for 7 days. Water was provided *ad libitum*. The study was carried out in accordance with the approved guidelines of the animal ethics committee, University of KwaZulu-Natal, Durban, South Africa (protocol approval number: AREC/020/017D).

Groupings

The animals were grouped into 6 consisting of Normal Control (NC): Normal rats (non-diabetic and not treated); Diabetic Control (DC): Diabetic and untreated control; Diabetic + low dose (DSG-LD): Diabetic rats administered low dose (150 mg/kg bodyweight [bw]) of RPW; Diabetic + high dose (DSG): Diabetic rats administered high dose (300 mg/kg bw) of RPW; Diabetic + standard drug metformin (DSM): Diabetic rats administered 200 mg/kg bw metformin; and Normal Toxicological Group (PHD): Non-diabetic rats administered high dose (300 mg/kg bw) of RPW.

Each group consists of 5 rats for normal groups, and 7 for the diabetics. The treatment design is summarized in Fig. 1.

Induction of type 2 diabetes

T2D was induced by first feeding 10% fructose solution to the animals in diabetic groups (DC, DSG-LD, DSG, and DSM) for 2 weeks *ad libitum*, before injecting (i.p) with streptozotocin (40 mg/kg BW) dissolved in citrate buffer

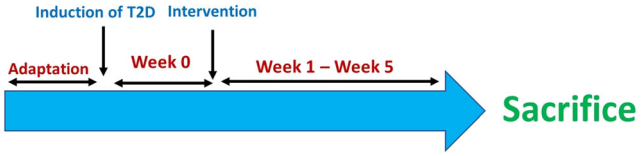

Fig. 1 Summary timeline of intervention trial

(pH 4.5) after an overnight fast. While the normal groups, NC and PHD were fed normal drinking water and injected (i.p) with citrate buffer only.

The rats were assessed for their non-fasting blood glucose (NFBG) levels after 7 days using a glucometer (Glucoplus Inc., Quebec, Canada). They were considered diabetic, with blood glucose level > 200 mg/dL.

Intervention trial

Raffia palm wine were orally administered to DSG-LD and DSG at low (150 mg/kg bw) and high (300 mg/kg bw) doses using a gastric gavage needle. PHD was administered 300 mg/kg bw of RPW, while NC and DC were administered distilled water only. The intervention period lasted for 5 weeks.

Collection of organs

At the end of the intervention trial, the rats were humanely sacrificed by euthanizing with halothane anesthesia. The brains were collected and washed in 0.9% NaCl and weighed. Parts of the cerebellum were excised and fixed in 10% neutral buffered formalin for histology and immunohistochemistry. About 2 mm of the cerebellum was also excised and fixed in 2.5% glutaraldehyde for electron microscopy. The remaining parts of the brain were homogenized in a homogenizing buffer (50 mM sodium phosphate buffer with 10% triton X-100, pH 7.5), and centrifuged at 15,000 rpm for 10 mins at 4 °C. The supernatants were decanted into 2 mL Eppendorf tubes and stored at −20 °C.

Determination of oxidative stress and proinflammatory biomarkers

Reduced glutathione (GSH) level

The GSH level was determined using the Ellman's method (Ellman 1959). Briefly, the supernatants were deproteinized with an equal volume of 10% TCA and then centrifuged at 3500 rpm for 5 mins at 25 °C. Thereafter, 200 μL of the supernatant was pipetted into a 96 well plate. A 50 μL of Ellman reagent was then added and allowed to stand for 5 mins. Absorbance was read at 415 nm. The GSH level was then extrapolated from the standard curve of plotted GSH concentrations.

Superoxide dismutase (SOD) activity

Superoxide dismutase activity was determined using previously established method which is based on the principle that H_2O_2 from SOD catalyzed dismutation of $O_2^{\cdot-}$ oxidizes 6-hydroxydopamine (6-HD) to produce a colored product (Gee and Davison 1989). Briefly, 170 μL of 0.1 mM diethylenetriaminepentaacetic acid (DETAPAC) and 15 μL of the samples were added in the each well of a 96-well plate. Thereafter, 15 μL of 1.6 mM 6-HD was added and mixed by gently tapping all four sides of plates. Absorbance of the resultant mixture was measured at 492 nm for 5 mins at 1 min interval.

Catalase activity

The catalase activity of the supernatants was calculated using previously established protocol (Aebi 1984). Briefly, 340 μL of 50 mM sodium phosphate buffer (pH 7.0) was mixed with 10 μL of the supernatants, 150 μL of 2 M H_2O_2 was then added to the mixture. Absorbance was read at 240 nm for 3 min at 1 min interval.

Lipid peroxidation levels

Lipid peroxidation levels of the supernatants were determined by measuring thiobarbituric acid reactive substances (TBARS), expressed as malondialdehyde (MDA) equivalent (Chowdhury and Soulsby 2002). Briefly, 100 μL of the supernatants were mixed with an equal volume of 8.1% SDS solution, 375 μL of 20% acetic acid, 1 mL of 0.25% thiobarbituric acid (TBA), and 425 μL of distilled water. The reaction mixture was heated at 95 °C for 1 h in a water bath. Thereafter, 200 μL of the heated mixture was pipetted into 96-well plate and absorbance read at 532 nm.

Myeloperoxidase activity

The myeloperoxidase (MPO) activities of the supernatants were determined using a previously established method with slight modifications (Granell et al. 2003). Briefly, 100 μL of the samples or distilled water (blank) were incubated with 100 μL of 5 mM KCl and 25 μL of 2 M H_2O_2 for 10 mins. Thereafter, 50 μL of 1.25% ammonium molybdate was added to the reaction mixture and allowed to stand for 5 mins. Absorbance was read at 405.

Determination of ATPase activity

The ATPase activities of the supernatants were analyzed using previously described protocol with slight modification (Adewoye et al. 2000; Erukainure et al. 2017). Briefly,

200 μL of the supernatants were incubated with 200 μL of 5 mM KCl, 1300 μL of 0.1 M Tris-HCl buffer, and 40 μL of 50 mM ATP at 37 °C in a shaker for 30 mins. Thereafter, 1 mL of distilled water and 1.25% ammonium molybdate were added respectively to stop the reaction. 1 mL of freshly prepared 9% ascorbic acid was then added to the reaction mixture and allowed to stand for 30 mins. Absorbance was read at 660 nm and ATPase activity was calculated as the amount of inorganic phosphate (Pi) released/min/mg protein.

Determination of acetylcholinesterase activity

The Ellman's method was utilized in determining the acetylcholinesterase activities of the supernatants (Ellman et al. 1961). Briefly, 20 μL of the supernatant was mixed with 10 μL of 3.3 mM Ellman's reagent (pH 7.0) and incubated with 50 μL of 0.1 M phosphate buffer (pH 8) for 20 min at 25 °C. 10 μL of 0.05 M acetylcholine iodide was then added to the reaction mixture and absorbance read at 412 nm at 3 min intervals.

Histology

The fixed cerebellar tissues were subjected to paraffin embedding using standard protocol, before staining with hematoxylin and eosin. A Leica slide scanner (SCN 4000, Leica-biosystems Germany) was used in viewing the slides.

Scanning Electron microscopy

Microscopic analysis of the cerebellar cortex was carried out with a scanning electron microscope (SEM; Zeiss Ultra Plus). The fixed tissues were buffer-washed thrice at 5 mins intervals to remove glutaraldehyde. They were post-fixed with 0.5% osmium tetraoxide for 2 h. The tissues were washed with distilled water thrice at 5 mins interval, before subjecting to dehydration using ethanol of increasing concentrations: 25% (twice at 5 mins interval), 50% (twice at 5 mins interval), 75% (twice at 5 mins interval) and 100% (twice at 10 mins interval). The tissue samples were dried in a critical-point-dryer apparatus, gold coated, and observed at an accelerating voltage of 20–25 k with a SEM (Zeiss Ultra Plus).

Energy dispersive X-ray (EDX) microanalysis

After SEM analysis, the cerebellar samples were further analyzed for elemental distributions by energy dispersive X-ray (EDX) microanalysis using a SEM (Zeiss Ultra Plus) equipped with an Oxford Instruments X-Max 80 mm2 Solid State EDX detector.

Immunohistochemistry

Thin sections of 5 μm thickness were obtained from routine paraffin embedded tissues prepared during histology. Following deparaffinization, sections were subjected to antigen retrieval by heating in a citrate-based antigen unmasking solution, pH 6.0 (Vector®, Burlingame, CA, USA; #H3300) for 30 mins in a steamer and cooled on the bench at room temperature for 30 mins. Endogenous peroxidase blocking was performed in 0.3% hydrogen peroxide in Tris Buffered Saline (TBS, pH 7.4) for 10 mins. Sections were blocked in 2.5% normal horse serum (Vector® #MP-7401) for 20 mins. Sections were then incubated overnight at 4 °C in primary rabbit antibodies: Nrf2 (Abcam, MA, USA; #ab31163) at 1:100 dilution. Sections were washed in TBS and incubated in ImmPRESS™ HRP Anti-Rabbit IgG (Peroxidase) Polymer Reagent, made in horse (Vector® #MP-7401). Colour was developed with DAB Peroxidase (HRP) Substrate Kit (Vector® #SK-4100), and sections were counter-stained in Harris hematoxylin. Sections without primary antibodies were similarly processed to control for binding of the secondary antibody. No specific immunoreactivity was detected on these control sections. Immunostained sections were digitized with a Pannoramic 250 Flash II slide scanner (3D Histech, Budapest, Hungary) and representative photomicrographs were obtained at 200x magnification using 3DHistech Case Viewer Software. Image analysis was performed using ImmunoRatio plugin on Image J software (NIH, USA), which separates and quantifies the percentage of DAB (positive immunoreactivity) by digital color deconvolution (Tuominen et al. 2010).

Glucose uptake in rat brain ex vivo

This was carried out by incubating freshly harvested normal rats' (SD strain, male) brains with different concentrations of RPW (30, 60, 120 and 240 μg/mL) in 8 mL of Krebs buffer containing 11.1 mM glucose for 2 h under conditions of 5% CO_2, 95% oxygen and 37 °C (Chukwuma and Islam 2015). An extra incubation without any treatment served as a control, while metformin served as the standard antidiabetic drug. Prior to incubation, an aliquot of the buffer was collected in 2 mL micro tubes for uptake analysis.

After incubation, the glucose concentrations of the buffer collected before and after incubation were analyzed with an automated chemistry analyzer (Labmax Plenno, Labtest Inc., Lagoa Santa, Brazil). Glucose uptake was calculated using the formula:

$$Glucose\ uptake = \frac{GC1 - GC2}{Weight\ of\ brain\ tissue\ (g)}$$

Where GC1 and GC2 are glucose concentrations (mg/dL) before and after incubation, respectively.

Statistical analysis

Data obtained were analyzed with one-way analysis of variance (ANOVA) and significant difference established at $p < 0.05$, with results reported as mean ± SD. Tukey's HSD-multiple range post hoc test was used to find the significance of difference. All statistical analyses were carried out using IBM SPSS for Windows, version 23.0 (SPSS Inc., Chicago, IL) and Microsoft 2016 Excel spread sheet.

Results

There was an elevation of blood glucose level on induction of T2D. The level was however, reduced by 44.29 and 53.57% after treatment with low and high dose of RPW, respectively.

Oxidative biomarkers were measured in order to determine the oxidative stress levels in the brain tissues of the experimental animals. As shown in Figs. 2a, 2d, induction of T2D led to a significant ($p < 0.05$) decrease in GSH levels, SOD and catalase activities, with concomitant increase in MDA levels. These were reversed on treatment with RPW and metformin to levels indistinguishable from controls. Administration of RPW to normal rats had no significant effect on GSH levels and SOD activities but reduced the catalase activity compared to the control. These results indicate the potent antioxidant activity of RPW.

Myeloperoxidase activity was measured in order to determine the level of proinflammation in the brain tissues of the experimental animals. Induction of T2D led to a significant ($p < 0.05$) increase in myeloperoxidase activity as shown in Fig. 3, indicating a proinflammatory response. This was significantly reduced in the RPW treated groups, with low dose showing the better activity, which is comparable with metformin. RPW had no significant effect on the activity in normal rats compared to the control.

ATPase activity was measured in order to have an insight on the ATP levels in brain tissues of the experimental animals. As shown in Fig. 4, ATPase activity in the diabetic group was significantly ($p < 0.05$) higher compared to the control. This effect was attenuated in response to the treatment with RPW, while the high dose showed a marked reduction reaching levels indistinguishable from controls. Metformin had no significant effect on the activity. The activity significantly increased in normal rats administered RPW compared to respective controls.

Acetylcholinesterase activity was measured in the brain tissues of the experimental animals in order to determine the inhibitory effect of RPW on the enzyme. Induction of T2D led to significant ($p < 0.05$) increase in acetylcholinesterase activity as depicted in Fig. 5. This effect was significantly reduced in rats treated with low dose of RPW. The metformin treated group, DSM also showed a significant reduction in acetylcholinesterase activity. Acetylcholinesterase activity in normal

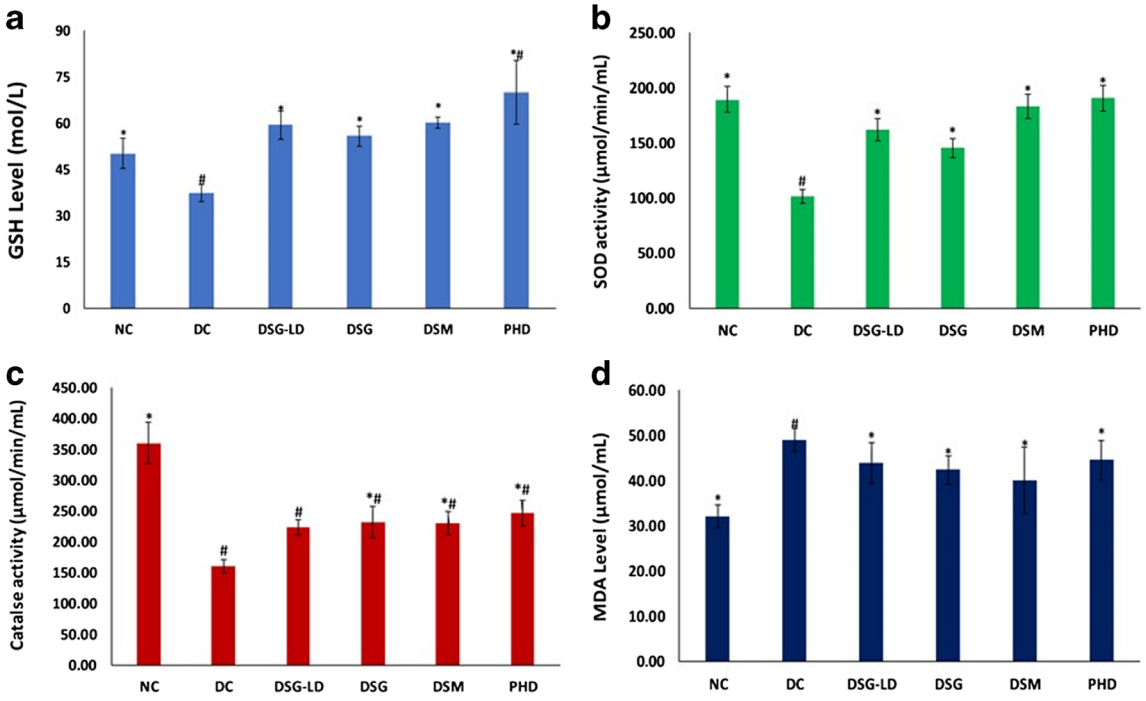

Fig. 2 Antioxidant status of different animal groups at the end of the intervention period. Values = mean ± SD; $n = 5$ (NC and PHD) and 7 (DC, DSG-LD, DG, and DSM). *Statistically ($p < 0.05$) significant to DC, #statistically significant ($p < 0.05$) to NC. **NC** = normal rats, **DC** = diabetic control, **DSG-LD** = diabetic rats + Raffia palm wine (150 mg/kg bw), **DSG** = diabetic rats + Raffia palm wine (300 mg/kg bw), **DSM** = diabetic rats + metformin (200 mg/kg bw), and **PHD** = Normal rats + Raffia palm wine (300 mg/kg bw)

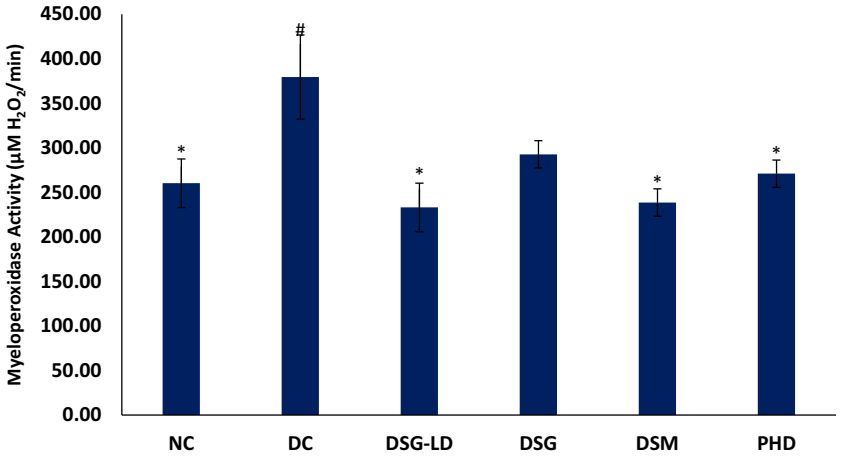

Fig. 3 Myeloperoxidase activities of experimental groups. Values = mean ± SD; n = 5 (NC and PHD) and 7 (DC, DSG-LD, DG, and DSM). *Statistically ($p < 0.05$) significant to DC, #statistically significant ($p < 0.05$) to NC. **NC** = normal rats, **DC** = diabetic control, **DSG-LD** = diabetic rats + Raffia palm wine (150 mg/kg bw), **DSG** = diabetic rats + Raffia palm wine (300 mg/kg bw), **DSM** = diabetic rats + metformin (200 mg/kg bw), and **PHD** = Normal rats + Raffia palm wine (300 mg/kg bw)

rats administered RPW was indistinguishable from the normal control group.

Histological analyses were carried out in order to reveal the morphology of the cerebellar cortices of the experimental animals. Histological analysis of the cerebellar cortex revealed intact Purkinje and granular cell layers as shown in Fig. 6a. The intactness of these layers was distorted upon induction of T2D (Fig. 6b), with evidence for compromised neuronal integrity. These layers appeared normal in rats treated with low dose of RPW and metformin (Fig. 6c, e), indicating a protective activity and maintenance of optimal neuronal integrity.

The cerebellar cortices of the experimental animals were subjected SEM analysis in order to reveal the surface morphology and neuronal distributions. SEM analysis of the cerebellar cortex revealed intact Purkinje and glial cells, with a vast network of dendrites and axons (Fig. 7a). This intactness was also distorted in the untreated diabetic group (Fig. 7b) as evidenced by a depleted number of Purkinje and glial cells, and altered network of dendrites and axons. The dendrites and axon networks were more conspicuous in the low dose RPW treated group (Fig. 7c), while the Purkinje and glial cells, and nerve networks were more intact in the high dose treated group (Fig. 7d). These cells and networks were altered in metformin treated rats (Fig. 7e). Administration of RPW to normal rats had no discernible effect on the Purkinje and glial cells as well as dendrites and axons networks (Fig. 7f).

EDX mapping of the cerebellar cortices was carried out in order to determine the elemental distribution in the cortices of the experimental animals. Figure 8a reveals the EDX mapping of the cerebellar cortex, showing elemental distribution in the cortex. Quantitative analysis revealed depleted levels of carbon, nitrogen and iron, with concomitantly elevated levels of

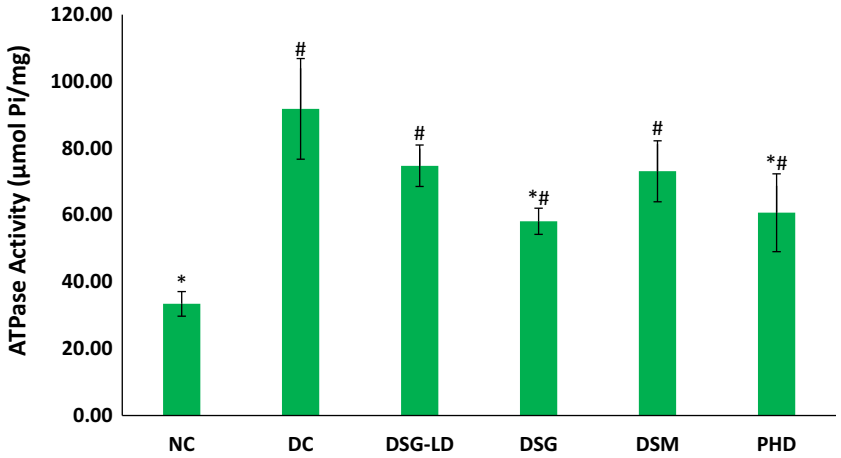

Fig. 4 ATPase activities of experimental groups. Values = mean ± SD; n = 5 (NC and PHD) and 7 (DC, DSG-LD, DG, and DSM). *Statistically ($p < 0.05$) significant to DC, #statistically significant ($p < 0.05$) to NC. **NC** = normal rats, **DC** = diabetic control, **DSG-LD** = diabetic rats + Raffia palm wine (150 mg/kg bw), **DSG** = diabetic rats + Raffia palm wine (300 mg/kg bw), **DSM** = diabetic rats + metformin (200 mg/kg bw), and **PHD** = Normal rats + Raffia palm wine (300 mg/kg bw)

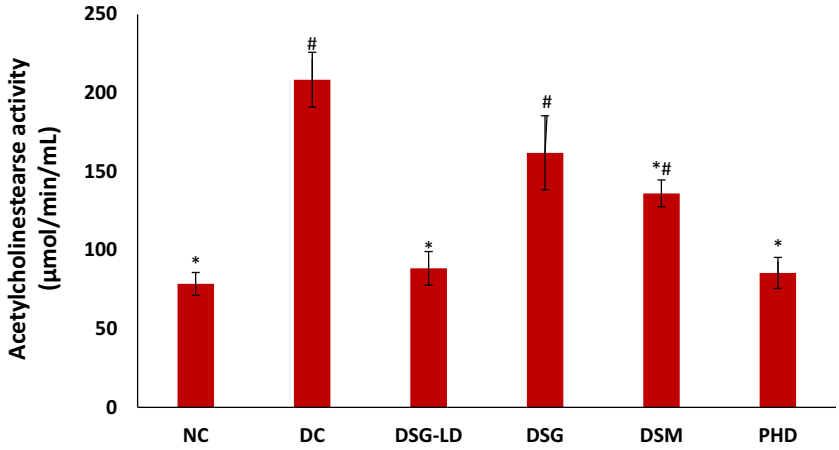

Fig. 5 Acetylcholinesterase activities of experimental groups. Values = mean ± SD; n = 5 (NC and PHD) and 7 (DC, DSG-LD, DG, and DSM). *Statistically ($p < 0.05$) significant to DC, #statistically significant ($p < 0.05$) to NC. **NC** = normal rats, **DC** = diabetic control, **DSG-LD** = diabetic rats + Raffia palm wine (150 mg/kg bw), **DSG** = diabetic rats + Raffia palm wine (300 mg/kg bw), **DSM** = diabetic rats + metformin (200 mg/kg bw), and **PHD** = Normal rats + Raffia palm wine (300 mg/kg bw)

oxygen, magnesium, aluminum and calcium (Fig. 8b). Induction of T2D had little or no effect on the cerebellar potassium content. These were reversed in the RPW treated rats, with the low dose showing elevated levels of carbon and

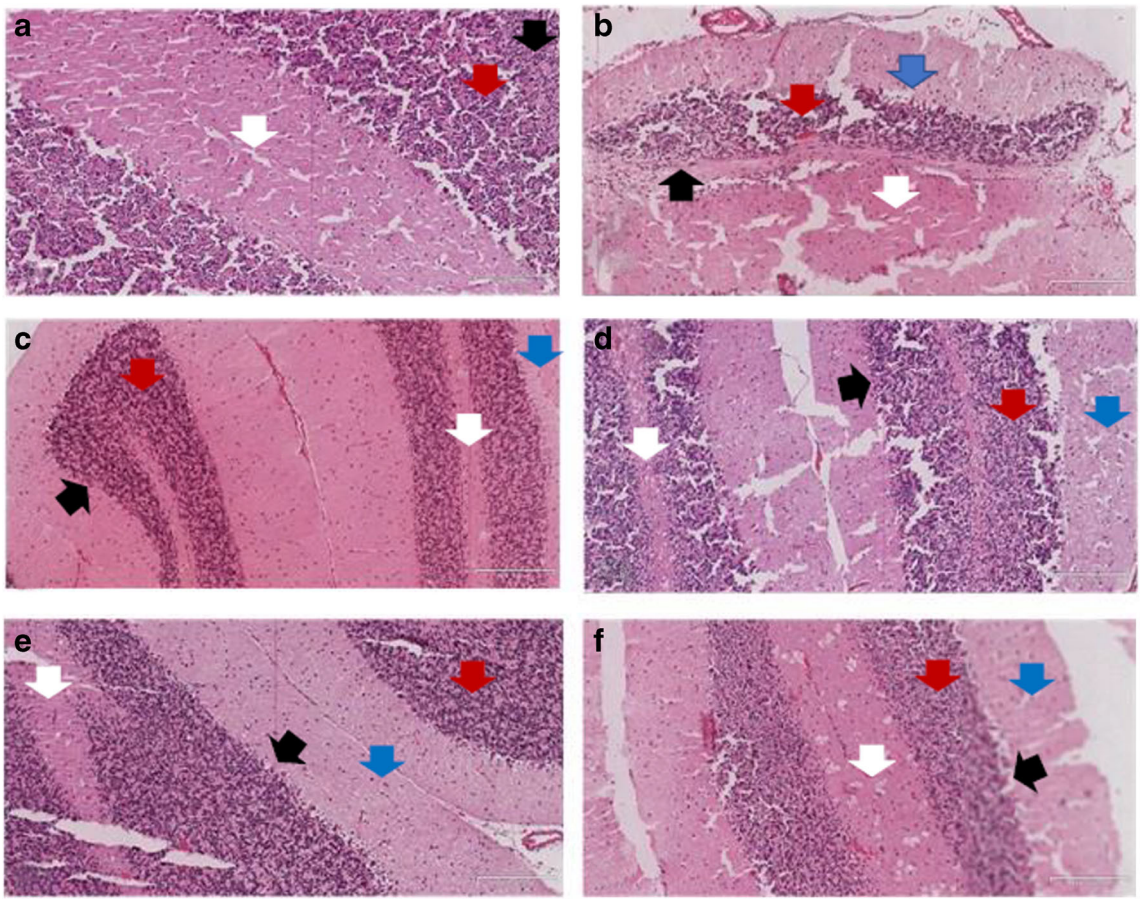

Fig. 6 Morphological changes in cerebellar tissues of experimental groups. Magnification: 10x – 0.02. (A) = NC, (B) = DC, (C) = DSG-LD, (D) = DSG, (E) = DSM, and (F) = PHD. **Legends**: Black arrow = Purkinje cell layer; Red arrow: Granule cell layer; White arrow: white matter; Blue arrow: Molecular layer. **NC** = normal rats, **DC** = diabetic control, **DSG-LD** = diabetic rats + Raffia palm wine (150 mg/kg bw), **DSG** = diabetic rats + Raffia palm wine (300 mg/kg bw), **DSM** = diabetic rats + metformin (200 mg/kg bw), and **PHD** = Normal rats + Raffia palm wine (300 mg/kg bw)

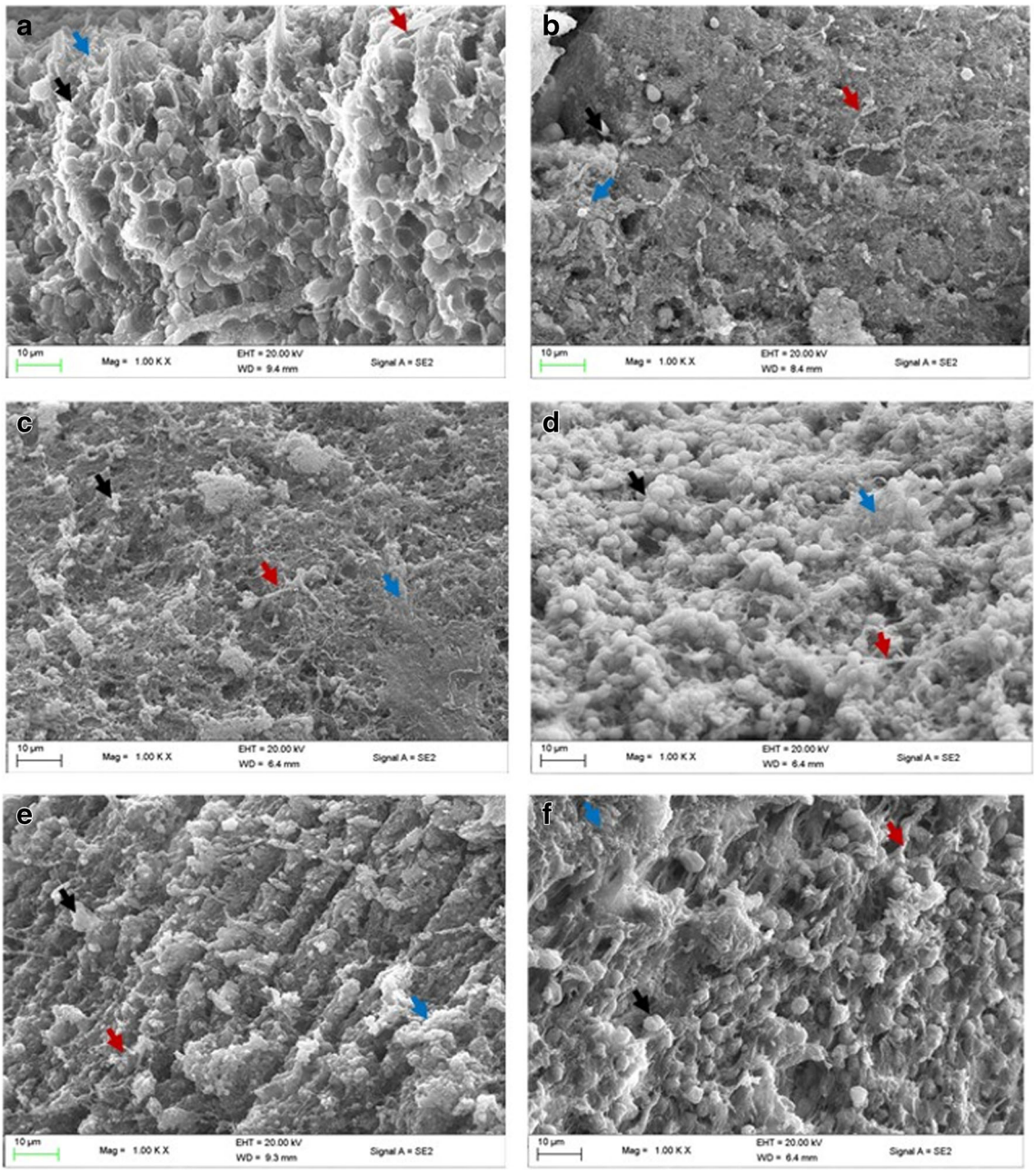

Fig. 7 SEM analysis of cerebellar tissues of experimental groups. Magnification = 1000x. (A) = NC, (B) = DC, (C) = DSG-LD, (D) = DSG, (E) = DSM, and (F) = PHD. **Legend:** Black arrow = Purkinje cells; Blue arrow = dendrite network; Red arrow = axon. **NC** = normal rats, **DC** = diabetic control, **DSG-LD** = diabetic rats + Raffia palm wine (150 mg/kg bw), **DSG** = diabetic rats + Raffia palm wine (300 mg/kg bw), **DSM** = diabetic rats + metformin (200 mg/kg bw), and **PHD** = Normal rats + Raffia palm wine (300 mg/kg bw)

iron, and depleted levels of potassium. While the high dose showed higher levels of nitrogen and potassium compared to the control. Magnesium, calcium and iron were largely depleted in the cerebellar cortex of diabetic rats treated with high dose of RPW. The cerebellar aluminum contents were highly depleted in diabetic rats treated with both doses of RPW.

The expression of Nrf2 was determined in the cerebellar cortices of the experimental animals in order to investigate the suppressive effect of RPW on the expression in T2D. Induction of T2D led to significantly ($P < 0.05$) increased expression of Nrf2 in the cerebellar cortex, particularly in the Purkinje and granular cell layers compared to the normal controls, (NC). Treatment with RPW attenuated the increase in Nrf2 expression in T2D rats (Fig. 9).

Ex vivo glucose uptake was carried out in order to determine the ability of RPW to stimulate brain glucose uptake. Incubation of rat brain with RPW led to decreased glucose level of the incubating buffer, suggesting increased glucose uptake, as depicted in Fig. 10. This enhanced glucose uptake activity increased in a concentration-dependent manner.

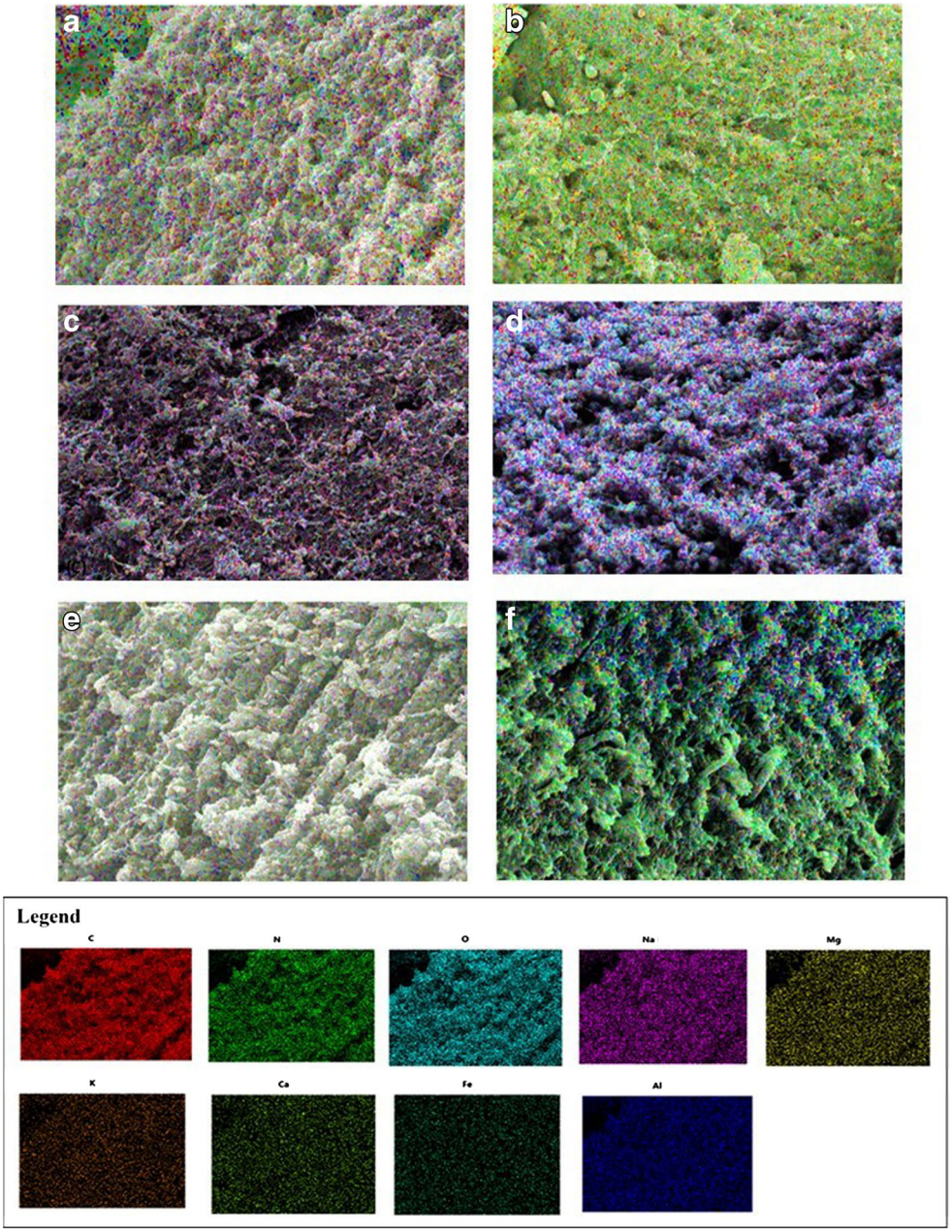

Fig. 8 **A.** EDX mapping of cerebellar tissues of experimental groups. Magnification = 1000x. (**a**) = NC, (**b**) = DC, (**c**) = DSG-LD, (**d**) = DSG, (**e**) = DSM, and (**f**) = PHD. **Legends:** C = carbon, N = nitrogen, O = oxygen, Na = sodium, Mg = magnesium, K = potassium, Ca = calcium, Fe = iron, and Al = aluminum. **NC** = normal rats, **DC** = diabetic control, **DSG-LD** = diabetic rats + Raffia palm wine (150 mg/kg bw), **DSG** = diabetic rats + Raffia palm wine (300 mg/kg bw), **DSM** = diabetic rats + metformin (200 mg/kg bw), and **PHD** = Normal rats + Raffia palm wine (300 mg/kg bw). **B.** Quantitative analysis of EDX scans

Incubation with metformin did not alter glucose uptake vs. control.

Discussion

The brain dependence on glucose as its primary source of energy is well established, with neurons being the highest consumers owing to their high energy demand (Howarth et al. 2012; Mergenthaler et al. 2013). Hence, the continuous need for a constant supply of glucose from the blood across the BBB to the brain via glucose transporters. This supply has been reported to be altered in T2D (Vagelatos and Eslick 2013; Whitlow et al. 2015), and has been attributed to down regulation of glucose transporters at the BBB (Gejl et al. 2017; Hwang et al. 2017). Diminished brain supply of glucose

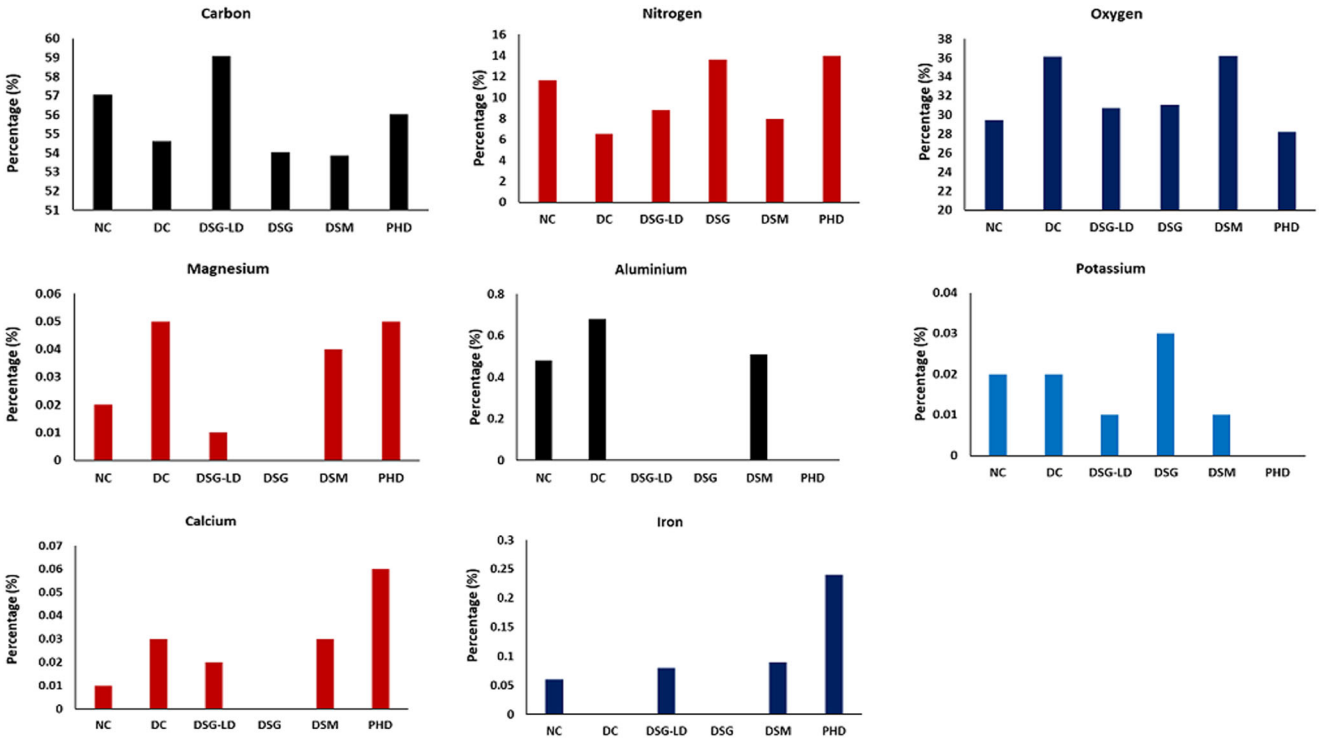

Fig. 8 (continued)

might, in turn, lead to neurodegenerative diseases characterized by oxidative stress, defective physiology, neuronal loss and dysfunction. In this study, the therapeutic effect of RPW on T2D-induced oxidative brain injury as well as its ability to promote brain glucose uptake ex vivo were investigated.

The high consumption of O_2 and concomitant dependence on glucose by the brain has been attributed for its high susceptibility to oxidative stress, which has been recognized as a major mechanism of T2D-induced neurodegeneration (Das et al. 2009; Patel 2016). This susceptibility can also be attributed to its low endogenous antioxidative system, high polyunsaturated fatty acid content, as well as the excitotoxic and auto-oxidizable activities of neurotransmitters (Patel 2016). The depleted GSH level, SOD and catalase activities upon induction of T2D (Figs. 2a, c) portray a distorted pro-oxidant/antioxidant equilibrium, reflected by increased ROS production. This corroborates earlier reports on the increased activities of these biomarkers in brain tissues of STZ-induced diabetic rats (Mastrocola et al. 2005; Moreira et al. 2003). ROS, such as $O_2^{\bullet-}$ and. OH are toxic to neuronal cells (Uttara et al. 2009). SOD catalyzes the dismutation of $O_2^{\bullet-}$ to H_2O_2 and O_2. Catalase further catalyzes the breakdown of H_2O_2 to H_2O and O_2 (Erukainure et al. 2017). In the absence of its breakdown by catalase, H_2O_2 generates hydroxyl ions ($^{\bullet}OH$). Both H_2O_2 and $^{\bullet}OH$ can initiate peroxidation of polyunsaturated fatty acids. The elevated MDA level in brain tissues of the diabetic control (DC) rats (Fig. 2d) indicate the occurrence of lipid peroxidation, which correlates with the depleted GSH levels, SOD and catalase activities. H_2O_2 can also be converted to hypochlorite (HOCl) in a reaction catalyzed myeloperoxidase in the presence of hydrochloric acid (HCl) (Patel 2016). HOCl is known to have proinflammatory activities (Erukainure et al. 2018a). The increased myeloperoxidase activity in the untreated diabetic group (DC) (Fig. 3), may thus reflect a proinflammatory activity. The reversal of these levels and activities to near normal in the RPW-treated groups, indicates an antioxidative and anti-proinflammatory potential of the palm wine.

Altered ATP levels have been reported in neurodegenerative diseases (Mochel et al. 2012; Zhang et al. 2015), as a consequence of increased ATPase activity. Increased brain ATPase also been implicated in impaired glucose facilitative transportation across the BBB (Falkowska et al. 2015; Magistretti and Allaman 2015). In this study, the increased ATPase activity in the diabetic control (DC) (Fig. 4) may insinuate an impaired glucose transport across the BBB and/or altered brain ATP concentration. The decreased activity in the treated groups, particularly DSG likely reflects increased ATP concentration as well as increased glucose uptake. This corroborates the increased glucose uptake in rat brains incubated with RPW in the presence of glucose (Fig. 10). The slight decrease in ATPase activities in brains of metformin-treated rats might be attributed to the fact that metformin activates GLUTs 2 and 4, which are less concentrated at the BBB (Kellett and Brot-Laroche 2005; Rice et al. 2011). This may also explain its lesser effect on brain glucose uptake (Fig. 10).

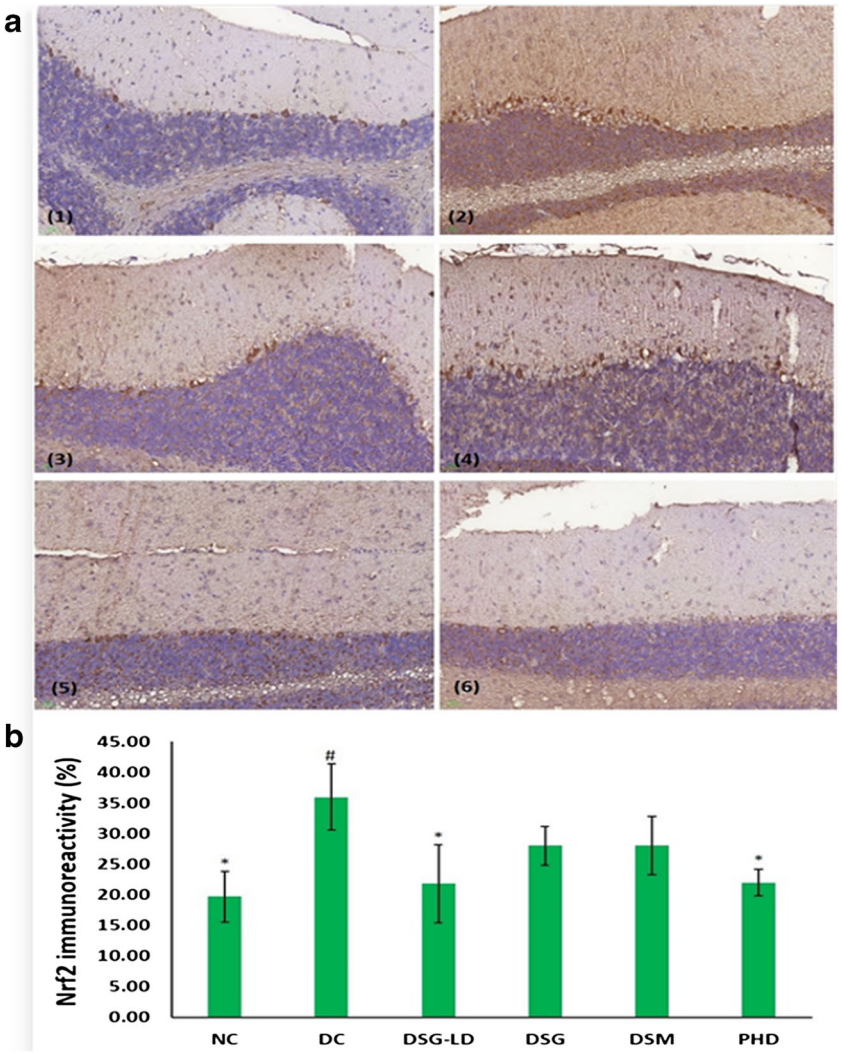

Fig. 9 **a**. Immunohistochemistry photomicrographs of Nrf2 expression in cerebellar cortex of experimental groups. Magnification = 200x; (1) = NC, (2) = DC, (3) = DSG-LD, (4) = DSG, (5) = DSM, and (6) = PHD. **b.** Nrf2 immunoreactivity in cerebellar cortex of experimental groups. *Statistically ($p < 0.05$) significant to DC, #statistically significant ($p < 0.05$) to NC. **NC** = normal rats, **DC** = diabetic control, **DSG-LD** = diabetic rats + Raffia palm wine (150 mg/kg bw), **DSG** = diabetic rats + Raffia palm wine (300 mg/kg bw), **DSM** = diabetic rats + metformin (200 mg/kg bw), and **PHD** = Normal rats + Raffia palm wine (300 mg/kg bw)

The role of acetylcholinesterase in exacerbating neurodegenerative diseases has been well established (Kuhl et al. 1999; Mushtaq et al. 2014; Pavlov et al. 2009). Its hydrolyzing effect on the neurotransmitter has been implicated in impaired cognition, pathogenesis and progression of Alzheimer disease, and motor neuron dysfunction amongst other neurodegenerative diseases (Hwang et al. 1999; Kuhad et al. 2008; Tabet 2006). Increased acetylcholinesterase activity has been reported in diabetic rat brains (Ghareeb and Hussen 2008; Kuhad et al. 2008), correlating with the increased activity in

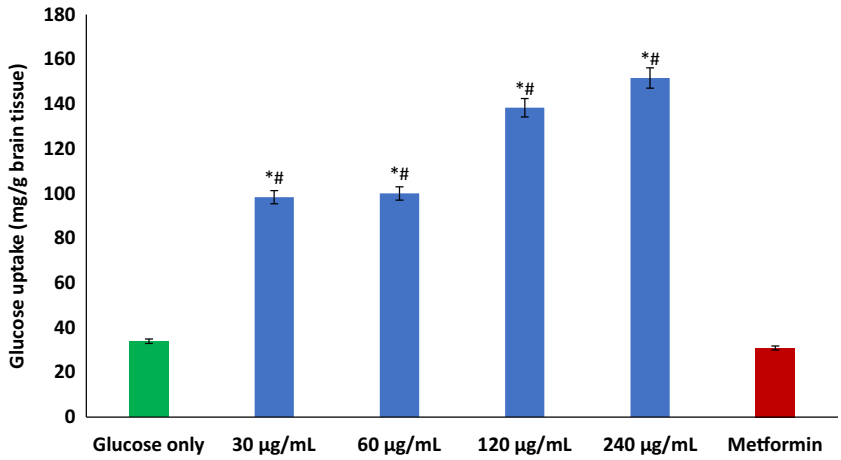

Fig. 10 Effect of Raffia palm wine on brain glucose uptake ex vivo. Values = mean ± SD; $n = 3$. *Statistically ($p < 0.05$) significant to metformin, #statistically significant ($p < 0.05$) to glucose only

the diabetic control in our present study (Fig. 5). The increased activity further corroborates an occurrence of brain injury due to induction of T2D. The increased activity also corroborates the increased myeloperoxidase activity (Fig. 3), as acetylcholinesterase activity has been correlated with the inhibition of the cholinergic anti-inflammatory pathways (Martelli et al. 2014; Pavlov et al. 2009). Increased oxidative stress has also been correlated with elevated acetylcholinesterase activity (Melo et al. 2003; Mushtaq et al. 2014), thereby implying that the increased acetylcholinesterase activity is consistent with increased oxidative stress (Fig. 2). The decreased acetylcholinesterase activities in treated diabetic rats, particularly the low dose RPW treated group, DSG-LD indicates an acetylcholinesterase-inhibitory activity as well as a protective effect against hyperglycemia-induced neurodegeneration by RPW. The reduced inhibitory effect of the high dose of RPW may be attributed to (1) the alteration of its pharmacokinetics at high dose; and/or (2) the target site of action may only accommodate a certain dose of drug or extract, which could suppress the effect of high doses.

Changes in brain morphology have been correlated with the pathogenesis and progression of most neurodegenerative diseases, with oxidative stress playing a major role (Ojo et al. 2014; Sidhu and Nehru 2004). The cerebellum controls motor and muscular activities in the brains as well as body balance (Imosemi 2013), with Purkinje cells as the main neurons present (Lopez et al. 2009). The morphological changes in the cerebellar cortex of the diabetic control rats (Fig. 6) as depicted by distorted Purkinje and granular cell layers indicate brain injury, which can be attributed to the T2D induced oxidative stress (Fig. 2). The vulnerability of Purkinje cells to oxidative stress has been reported (Chen et al. 2003; Kern and Jones 2006; Lopez et al. 2009). Their altered morphology and distribution has also been reported in diabetes (Solmaz et al. 2017; Yamano et al. 1986). This is further evident in the altered distribution and loss of Purkinje and glial cells as well as dendrites and axons networks as revealed in Fig. 7b. These changes indicate an altered neuronal integrity, which is common in most neurodegenerative diseases such as Alzheimer's disease. These results are in consent with reports on the alteration of cerebellar cortex on induction of DM in rats (Hernández-Fonseca et al. 2009; Nagayach et al. 2014; Ozdemir et al. 2016). The near-intactness of these cells and networks in the treated groups (Figs. 6c, 6f and 7c, 7f), particularly diabetic rats treated with RPW correlates with the observed antioxidant activities (Fig. 2). Thus, indicating a neuro-protective potential of RPW against T2D-induced neurodegeneration.

Altered elemental distribution, particularly accumulation of metals has been implicated in oxidative neurodegeneration (Chen et al. 2016; Jan et al. 2015). Unless altered, these metals are involved in the normal physiology of the brain as they act as co-factors for most enzymes and are integral component of most redox reactions (Uttara et al. 2009). Altered elemental distributions and accumulations have been reported in cerebellar toxicity (Folarin et al. 2017; Kamal and Kamal 2013). The increased O_2 content (Fig. 8) correlates with the induced oxidative stress in DC, as oxygen is the major precursor of ROS and its increased accumulation may lead to generation of $O_2^{\cdot-}$ (Patel 2016). The increased Ca and Al contents (Fig. 8) portrays toxic effect as their accumulation have been implicated in the pathogenesis and progression of neurodegeneration (Kamal and Kamal 2013; Wojda et al. 2008). The role of magnesium in neurodegeneration is still debatable. However, its aggravative and negative effect on neurodegeneration has been reported (Van Den Van Den Heuvel and Vink 2004). The modulation of these elemental levels to near normal in the treated groups, further portrays the neuro-protective effects of RPW.

Exacerbated Nrf2 expression has been implicated in the onset of T2D and antioxidant suppression, leading to ROS generation (He et al. 2012; Miao et al. 2012). This correlates with the increased expression in Purkinje and granular layers in the cerebellar cortex of the diabetic control group (Fig. 9b). The increased expression also corroborates the diminished antioxidant enzymes (SOD and catalase) activities and lipid peroxidation in the diabetic control (Fig. 2). The down regulation of the expressions particularly in rats treated with RPW, indicates an extenuative effect on cerebellar Nrf2 expression. This extenuative effect also corroborates the exacerbated antioxidative activity in the rat brains (Fig. 2).

Conclusion

These results indicate the neuroprotective potentials of RPW against oxidative brain injury in T2D. This is evident by its ability to reduce blood glucose level, attenuate oxidative stress and proinflammation, inhibit acetylcholinesterase and ATPase activities; modulate elemental distribution, attenuation of Nrf2 expression, with concomitant maintenance of cerebellum neuronal integrity, while stimulating brain glucose uptake.

Acknowledgments OE was supported by a competitive research grant from the Research Office, University of KwaZulu-Natal (UKZN), Durban, South Africa. OMI acknowledges the support of the 2017 IBRO-ISN Research Fellowship, and Analytical Imaging Facility, Albert Einstein College of Medicine USA (NCI: P30CA013330; SIG: #1S10OD019961-01). MA was supported by National Institute of Health (NIH) R01 ES10563, R01 ES07331 and R01 ES020852.

Compliance with ethical standards

Conflict of interest The authors report no conflict of interest.

References

Adewoye O, Bolarinwa A, Olorunsogo O (2000) Ca++, mg++-ATPase activity in insulin-dependent and non-insulin dependent diabetic Nigerians. Afr J Med Med Sci 29:195–199

Aebi H (1984) Catalase in vitro. Methods Enzymol 105:121–126

Barančík M, Grešová L, Barteková M, Dovinová I (2016) Nrf2 as a key player of redox regulation in cardiovascular diseases. Physiol Res 65 (Suppl. 1:S1–S10

Bassir O (1962) Observations on the fermentation of palm wine. West Afri J Biol Chem 6:20–25

Chen P, Peng C, Luff J, Spring K, Watters D, Bottle S, Furuya S, Lavin MF (2003) Oxidative stress is responsible for deficient survival and dendritogenesis in purkinje neurons from ataxia-telangiectasia mutated mutant mice. J Neurosci 23:11453–11460

Chen P, Miah MR, Aschner M (2016) Metals and neurodegeneration. F1000Research 5. https://doi.org/10.12688/f1000research.7431.1

Chowdhury P, Soulsby M (2002) Lipid peroxidation in rat brain is increased by simulated weightlessness and decreased by a soy-protein diet. Ann Clin Lab Sci 32:188–192

Chukwuma CI, Islam MS (2015) Effects of xylitol on carbohydrate digesting enzymes activity, intestinal glucose absorption and muscle glucose uptake: a multi-mode study. Food Funct 6:955–962

Cunningham A, Wehmeyer A (1988) Nutritional value of palm wine from Hyphaene coriacea and Phoenix reclinata (Arecaceae). Econ Bot 42: 301–306

Das S, Gautam N, Dey SK, Maiti T, Roy S (2009) Oxidative stress in the brain of nicotine-induced toxicity: protective role of Andrographis paniculata Nees and vitamin E. Appl Physiol Nutr Metab 34:124–135

Dieter BP (2014) Dysregulation of Nrf2 signaling in diabetes: an opportunity for a multi-target approach. J Diab Metab 6:2

Ellman GL (1959) Tissue sulfhydryl groups. Arch Biochem Biophys 82: 70–77

Ellman GL, Courtney KD, Andres V Jr, Featherstone RM (1961) A new and rapid colorimetric determination of acetylcholinesterase activity. Biochem Pharmacol 7:88–95

Erukainure OL, Mopuri R, Oyebode OA, Koorbanally NA, Islam MS (2017) Dacryodes edulis enhances antioxidant activities, suppresses DNA fragmentation in oxidative pancreatic and hepatic injuries; and inhibits carbohydrate digestive enzymes linked to type 2 diabetes. Biomed Pharmacother 96:37–47

Erukainure OL, Narainpersad N, Singh M, Olakunle S, Islam MS (2018a) Clerodendrum volubile inhibits key enzymes linked to type 2 diabetes but induces cytotoxicity in human embryonic kidney (HEK293) cells via exacerbated oxidative stress and proinflammation. Biomed Pharmacother 106:1144–1152

Erukainure OL, Oyebode OA, Chukwuma CI, Matsabisa MG, Koorbanally NA, Islam MS (2018b) Raffia palm (Raphia hookeri) wine inhibits glucose diffusion; improves antioxidative activities; and modulates dysregulated pathways and metabolites in oxidative pancreatic injury. J Food Biochem 43. https://doi.org/10.1111/jfbc.12749

Erukainure OL, Oyebode OA, Ijomone OM, Chukwuma CI, Koorbanally NA, Islam MS (2019a) Raffia palm (Raphia hookeri G. Mann & H. Wendl) wine modulates glucose homeostasis by enhancing insulin secretion and inhibiting redox imbalance in a rat model of diabetes induced by high fructose diet and streptozotocin. J Ethnopharmacol 237:159–170

Erukainure OL, Reddy R, Islam MS (2019b) Raffia palm (Raphia hookeri) wine extenuates redox imbalance and modulates activities of glycolytic and cholinergic enzymes in hyperglycemia induced testicular injury in type 2 diabetes rats. J Food Biochem 43. https://doi.org/10.1111/jfbc.12764

Eze MO, Ogan AU (1988) Sugars of the unfermented sap and the wine from the oil palm, Elaeis guinensis, tree. Plant Food Hum Nutr 38: 121–126

Ezeagu I, Fafunso M, Ejezie F (2003) Biochemical constituents of palmwine. Ecol Food Nutr 42:213–222

Falkowska A, Gutowska I, Goschorska M, Nowacki P, Chlubek D, Baranowska-Bosiacka I (2015) Energy metabolism of the brain, including the cooperation between astrocytes and neurons, especially in the context of glycogen metabolism. Int J Mol Sci 16:25959–25981

Folarin OR, Snyder AM, Peters DG, Olopade F, Connor JR, Olopade JO (2017) Brain metal distribution and neuro-inflammatory profiles after chronic vanadium administration and withdrawal in mice. Front Neuroanat 11:58

Gee P, Davison AJ (1989) Intermediates in the aerobic autoxidation of 6-hydroxydopamine: relative importance under different reaction conditions. Free Radic Biol Med 6(3):271–284

Gejl M, Brock B, Egefjord L, Vang K, Rungby J, Gjedde A (2017) Blood-brain glucose transfer in Alzheimer's disease: effect of GLP-1 analog treatment. Sci Report 7:17490

Ghareeb DA, Hussen HM (2008) Vanadium improves brain acetylcholinesterase activity on early stage alloxan-diabetic rats. Neurosci Lett 436:44–47

Granell S, Gironella M, Bulbena O, Panés J, Mauri M, Sabater L, Aparisi L, Gelpí E, Closa D (2003) Heparin mobilizes xanthine oxidase and induces lung inflammation in acute pancreatitis. Crit Care Med 31: 525–530

Gruca M, van Andel TR, Balslev H (2014) Ritual uses of palms in traditional medicine in sub-Saharan Africa: a review. J Ethnobiol Ethnomed 10:60

He H-J, Wang G-Y, Gao Y, Ling W-H, Yu Z-W, Jin T-R (2012) Curcumin attenuates Nrf2 signaling defect, oxidative stress in muscle and glucose intolerance in high fat diet-fed mice. World J Diabetes 3:94–104

Hernández-Fonseca JP, Rincón J, Pedreañez A, Viera N, Arcaya JL, Carrizo E, Mosquera J (2009) Structural and ultrastructural analysis of cerebral cortex, cerebellum, and hypothalamus from diabetic rats. Exper Diab Res 2009:1–12. https://doi.org/10.1155/2009/329632

Howarth C, Gleeson P, Attwell D (2012) Updated energy budgets for neural computation in the neocortex and cerebellum. J Cereb Blood Flow Metab 32:1222–1232

Hwang J-H, Hwang K-S, Leem J-K, Park P-H, Han S-M, Lee D-M (1999) The antiallodynic effects of intrathecal cholinesterase inhibitors in a rat model of neuropathic pain. Anesth J Amer Soc Anesth 90:492–499

Hwang JJ, Jiang L, Hamza M, Sanchez Rangel E, Dai F, Belfort-DeAguiar R, Parikh L, Koo BB, Rothman DL, Mason G, Sherwin RS (2017) Blunted rise in brain glucose levels during hyperglycemia in adults with obesity and T2DM. JCI Insight 2(20):e95913

Imosemi I (2013) The role of antioxidants in cerebellar development. A review of literature. Int J Morphol 31:203–210

Jan A, Azam M, Siddiqui K, Ali A, Choi I, Haq Q (2015) Heavy metals and human health: mechanistic insight into toxicity and counter defense system of antioxidants. Int J Mol Sci 16:29592–29630

Kamal I, Kamal H (2013) Effects of aluminum on rat cerebellar cortex and the possible protective role of Nigella sativa: a light and electron microscopic study. Egypt J Histol 36:979–990

Kellett GL, Brot-Laroche E (2005) Apical GLUT2: a major pathway of intestinal sugar absorption. Diabetes 54:3056–3062

Kern JK, Jones AM (2006) Evidence of toxicity, oxidative stress, and neuronal insult in autism. J Toxic Envir Heal Part B 9:485–499

Kim GH, Kim JE, Rhie SJ, Yoon S (2015) The role of oxidative stress in neurodegenerative diseases. Exper Neurobiol 24:325–340

Kosseva M, Joshi V, Panesar PS (2016) Science and Technology of Fruit Wine Production. Academic Press

Kuhad A, Sethi R, Chopra K (2008) Lycopene attenuates diabetes-associated cognitive decline in rats. Life Sci 83:128–134

Kuhl D et al. (1999) In vivo mapping of cerebral acetylcholinesterase activity in aging and Alzheimer's disease. Neurology 52:691–691, 699

Lopez IA, Acuna D, Beltran-Parrazal L, Lopez IE, Amarnani A, Cortes M, Edmond J (2009) Evidence for oxidative stress in the developing cerebellum of the rat after chronic mild carbon monoxide exposure (0.0025% in air). BMC Neurosci 10:53

Ma Q (2013) Role of nrf2 in oxidative stress and toxicity. Annu Rev Pharmacol Toxicol 53:401–426

Magistretti PJ, Allaman I (2015) A cellular perspective on brain energy metabolism and functional imaging. Neuron 86:883–901

Maritim A, Sanders R, Watkins J III (2003) Diabetes, oxidative stress, and antioxidants: a review. J Biochem Mol Toxicol 17:24–38

Martelli D, McKinley M, McAllen R (2014) The cholinergic anti-inflammatory pathway: a critical review. Auton Neurosci 182:65–69

Mastrocola R, Restivo F, Vercellinatto I, Danni O, Brignardello E, Aragno M, Boccuzzi G (2005) Oxidative and nitrosative stress in brain mitochondria of diabetic rats. J Endocrinol 187:37–44

McEwen BS, Reagan LP (2004) Glucose transporter expression in the central nervous system: relationship to synaptic function. Euro J Pharm 490:13–24

Melo JB, Agostinho P, Oliveira CR (2003) Involvement of oxidative stress in the enhancement of acetylcholinesterase activity induced by amyloid beta-peptide. Neurosci Res 45:117–127

Mergenthaler P, Lindauer U, Dienel GA, Meisel A (2013) Sugar for the brain: the role of glucose in physiological and pathological brain function. Trends Neurosci 36:587–597

Miao X, Bai Y, Sun W, Cui W, Xin Y, Wang Y, Tan Y, Miao L, Fu Y, Su G, Cai L (2012) Sulforaphane prevention of diabetes-induced aortic damage was associated with the up-regulation of Nrf2 and its down-stream antioxidants. Nutr Metab 9:84

Mochel F, Durant B, Meng X, O'Callaghan J, Yu H, Brouillet E, Wheeler VC, Humbert S, Schiffmann R, Durr A (2012) Early alterations of brain cellular energy homeostasis in Huntington disease models. J Biol Chem 287:1361–1370

Moreira PI, Santos MS, Moreno AM, Seiça R, Oliveira CR (2003) Increased vulnerability of brain mitochondria in diabetic (Goto-Kakizaki) rats with aging and amyloid-β exposure. Diabetes 52: 1449–1456

Mushtaq N, Schmatz R, Pereira LB, Ahmad M, Stefanello N, Vieira JM, Abdalla F, Rodrigues MV, Baldissarelli J, Pelinson LP, Dalenogare DP, Reichert KP, Dutra EM, Mulinacci N, Innocenti M, Bellumori M, Morsch VM, Schetinger MR (2014) Rosmarinic acid prevents lipid peroxidation and increase in acetylcholinesterase activity in brain of streptozotocin-induced diabetic rats. Cell Biochem Funct 32:287–293

Nagayach A, Patro N, Patro I (2014) Experimentally induced diabetes causes glial activation, glutamate toxicity and cellular damage leading to changes in motor function. Front Cell Neurosci 8:355

Nwaiwu O, Ibekwe VI, Amadi ES, Udebuani AC, Nwanebu FC, Oguoma OI, Nnokwe JC (2016) Evaluation of fermentation products of palm wine yeasts and role of Sacoglottis gabonensis supplement on products abundance. Beverages 2:9

Obahiagbon F, Osagie A (2007) Sugar and macrominerals composition of sap produced by Raphia hookeri palms. Afri J Biotech 6:744–750

Ojo O, Oyinloye B, Ajiboye B, Ojo A, Musa H, Olarewaju O (2014) Dichlorvos-induced oxidative stress in rat brain: protective effects of the ethanolic extract of Alstonia boonei stem bark. Asian J Pharm 8: 216–221

Okwu D, Nnamdi FU (2008) Evaluation of the chemical composition of Dacryodes edulis and Raphia hookeri Mann and Wendl exudates used in herbal medicine in south eastern Nigeria. Afri J Trad Compl Altern Med 5:194–200

Ozdemir NG, Akbas F, Kotil T, Yılmaz A (2016) Analysis of diabetes related cerebellar changes in streptozotocin-induced diabetic rats. Turk J Med Sci 46:1579–1592

Pardridge WM, Triguero D, Farrell CR (1990) Downregulation of blood-brain barrier glucose transporter in experimental diabetes. Diabetes 39:1040–1044

Patel M (2016) Targeting oxidative stress in central nervous system disorders. Trends Pharmacol Sci 37:768–778

Pavlov VA, Parrish WR, Rosas-Ballina M, Ochani M, Puerta M, Ochani K, Chavan S, al-Abed Y, Tracey KJ (2009) Brain acetylcholinesterase activity controls systemic cytokine levels through the cholinergic anti-inflammatory pathway. Brain Behav Immun 23:41–45

Rätsch C (2005) The encyclopedia of psychoactive plants: ethnopharmacology and its applications. Simon and Schuster

Reagan LP, Grillo CA, Piroli GG (2008) The as and ds of stress: metabolic, morphological and behavioral consequences. Eur J Pharmacol 585:64–75

Rice S, Pellatt LJ, Bryan SJ, Whitehead SA, Mason HD (2011) Action of metformin on the insulin-signaling pathway and on glucose transport in human granulosa cells. J Clin Endocrinol Metab 96:E427–E435

Sandberg M, Patil J, D'angelo B, Weber SG, Mallard C (2014) NRF2-regulation in brain health and disease: implication of cerebral inflammation. Neuropharmacology 79:298–306

Sidhu P, Nehru B (2004) Lead intoxication: histological and oxidative damage in rat cerebrum and cerebellum. J Trace Elem Exp Med 17: 45–53

Solmaz V, Köse Özlece H, Eroglu HA, Aktuğ H, Erbaş O, Taşkıran D (2017) Accumulation of α-Synuclein in cerebellar Purkinje cells of diabetic rats and its potential relationship with inflammation and oxidative stress markers. Neuro Res Inter 2017:5952149

Tabet N (2006) Acetylcholinesterase inhibitors for Alzheimer's disease: anti-inflammatories in acetylcholine clothing. Age Ageing 35:336–338

Tuley P (1965) Studies on the production of wine from the oil palm. J Nig Inst Oil Palm Res 4:283–289

Tuominen VJ, Ruotoistenmäki S, Viitanen A, Jumppanen M, Isola J (2010) ImmunoRatio: a publicly available web application for quantitative image analysis of estrogen receptor (ER), progesterone receptor (PR), and Ki-67. Breast Cancer Res 12:R56

Unnikrishnan R, Pradeepa R, Joshi SR, Mohan V (2017) Type 2 diabetes: demystifying the global epidemic. Diabetes 66:1432–1442

Uttara B, Singh AV, Zamboni P, Mahajan R (2009) Oxidative stress and neurodegenerative diseases: a review of upstream and downstream antioxidant therapeutic options. Current Neuropharma 7:65–74

Vagelatos NT, Eslick GD (2013) Type 2 diabetes as a risk factor for Alzheimer's disease: the confounders, interactions, and neuropathology associated with this relationship. Epidemiol Rev 35:152–160

van Crevel R, van de Vijver S, Moore DA (2017) The global diabetes epidemic: what does it mean for infectious diseases in tropical countries? Lancet Diabetes Endocrinol 5:457–468

Van Den Heuvel C, Vink R (2004) The role of magnesium in traumatic brain injury. Clin Calc 14:9–14

Whitlow C et al (2015) Effects of type 2 diabetes on brain structure and cognitive function: African American–diabetes heart study MIND. Ame J Neuroradiol 36:1648–1653

Wojda U, Salinska E, Kuznicki J (2008) Calcium ions in neuronal degeneration. IUBMB Life 60:575–590

Wrighten SA, Piroli GG, Grillo CA, Reagan LP (2009) A look inside the diabetic brain: contributors to diabetes-induced brain aging. Biochim Biophys Acta Mol basis Dis 1792:444–453

Yamano T, Shimada M, Fujizeki Y, Kawasaki H, Onaga A (1986) Quantitative synaptic changes on Purkinje cell dendritic spines of rats born from streptozotocin-induced diabetic mothers. Brain Dev 8:269–273

Zhang C, Rissman RA, Feng J (2015) Characterization of ATP alternations in an Alzheimer's disease transgenic mouse model. J Alzheimers Dis 44:375–378

Zucker SN, Fink EE, Bagati A, Mannava S, Bianchi-Smiraglia A, Bogner PN, Wawrzyniak JA, Foley C, Leonova KI, Grimm MJ, Moparthy K, Ionov Y, Wang J, Liu S, Sexton S, Kandel ES, Bakin AV, Zhang Y, Kaminski N, Segal BH, Nikiforov MA (2014) Nrf2 amplifies oxidative stress via induction of Klf9. Mol Cell 53:916–928